

(2)

DTIC FILE COPY

CEVANS/049/FR-9002

Final Report

AD-A219 203

SECONDARY ION MASS SPECTROMETRY CHARACTERIZATION  
OF IMPLANTS INTO GAAS AND GAP FOR WAVEGUIDES  
AND INTEGRATED OPTICS APPLICATIONS

Prepared by:

Robert S. Wilson, Ph.D.,  
Hughes Research Laboratories

for:

CHARLES EVANS & ASSOCIATES  
301 Chesapeake Drive  
Redwood City, CA 94063  
(415) 369-4567

Reporting Period: April 28, 1986 - October 30, 1989

Sponsored by:

Department of the Army  
United States Army Laboratory Command  
Army Research Office  
P. O. Box 12211  
Research Triangle Park, NC 27709-2211

ARO Proposal Number: 233240EL-S

Contract Number: DAAL03-86-C-0010

Principal Investigator:

  
Charles A. Evans, Jr., Ph.D.Effective Date of Contract: April 28, 1986  
Contract Expiration Date: October 30, 1989

January 10, 1990

DTIC  
ELECTE  
FEB 28 1990  
S B D  
PCAPPROVED FOR PUBLIC RELEASE;  
DISTRIBUTION UNLIMITED.

90 02 26 031

UNCLASSIFIED

SECURITY CLASSIFICATION OF THIS PAGE (When Data Entered)

REPORT DOCUMENTATION PAGE		READ INSTRUCTIONS BEFORE COMPLETING FORM
1. REPORT NUMBER	2. GOVT ACCESSION NO.	3. RECIPIENT'S CATALOG NUMBER
ARL 23324.1-ELS	N/A	N/A
4. TITLE (and Subtitle) Secondary Ion Mass Spectrometry Characterization of Implants into GaAs and GaP for Waveguides and Integrated Optics Applications		5. TYPE OF REPORT & PERIOD COVERED Final Report 86 APR 28 thru 89 OCT 30
7. AUTHOR(s) Robert S. Wilson. Ph.D.		6. PERFORMING ORG. REPORT NUMBER
9. PERFORMING ORGANIZATION NAME AND ADDRESS CHARLES EVANS & ASSOCIATES 301 Chesapeake Drive Redwood City, CA 94063		8. CONTRACT OR GRANT NUMBER(s) DAAL03-86-C-0010
11. CONTROLLING OFFICE NAME AND ADDRESS U. S. Army Research Office Post Office Box 12211 Research Triangle Park, NC 27709		10. PROGRAM ELEMENT, PROJECT, TASK AREA & WORK UNIT NUMBERS
14. MONITORING AGENCY NAME & ADDRESS (if different from Controlling Office)		12. REPORT DATE January 10, 1990
		13. NUMBER OF PAGES 35
		15. SECURITY CLASS. (of this report) Unclassified
		15a. DECLASSIFICATION DOWNGRADING SCHEDULE
16. DISTRIBUTION STATEMENT (of this Report)  Approved for public release; distribution unlimited.		
17. DISTRIBUTION STATEMENT (of the abstract entered in Block 20, if different from Report)  NA		
18. SUPPLEMENTARY NOTES  The view, opinions, and/or findings contained in this report are those of the author(s) and should not be construed as an official Department of the Army position, policy, or decision, unless so designated by other documentation.		
19. KEY WORDS (Continue on reverse side if necessary and identify by block number)  waveguides, ion implantation, optical waveguides, III-V compounds, diffusion, SIMS, secondary ion mass spectrometry, $\text{LiNbO}_3$		
20. ABSTRACT (Continue on reverse side if necessary and identify by block number) Hydrogen, He, and most dopant elements were implanted into GaAs, GaAsP, GaP, GaSb, InP, InAs, InSb, and $\text{LiNbO}_3$ at energies from 10 to 700 keV, and a few elements up to 2.4 MeV, in random and channeling orientations, annealed some of these implants, and measured their depth distributions using secondary ion mass spectrometry (SIMS). We calculated values of $R_p$ , $R_{\Delta R}$ , $\gamma_1$ , $\beta_2$ , using an LSS formulation, and using TRIM (for a few), a Monte Carlo calculation and measured these same profile parameters for the experimental profiles		

UNCLASSIFIED

SECURITY CLASSIFICATION OF THIS PAGE(When Data Entered)

BLOCK 20 (Continued)

using a Pearson IV computer fitting routine.

This work included studies of: characterization of Si implantation into GaAs in random and channeling orientations at energies from 10 keV to 6.0 MeV; a general description of as-implanted and annealed depth profiles of dopant implants (especially Be and Si) into GaP, GaAs, InP, and InSb; illustrations of the effects of heterostructures, including superlattices, on the redistribution of mobile impurities (H and Be) during thermal processing; brief illustrations of implants in other III-V technologies (GaAs/Si and GaAsP); lanthanide rare earth elements in III-V crystals; as-implanted and annealed MeV implants in III-V materials; characterization of proton exchanged  $\text{LiNbO}_3$ ; and redistribution of implanted H in  $\text{LiNbO}_3$ .

A significant result of this effort was the establishment of secondary ion mass spectrometry (SIMS) technologies for these materials. The use of our implants of known isotope and fluence provided calibration standards for the quantification of SIMS. We established SIMS relative sensitivity factors for both oxygen and cesium primary ion beams and positive and negative secondary ion mass spectrometry, using the variety of ions implanted. Another significant result of this research program was the measurement of range-energy and range straggle-energy tables and curves for the ions and materials studied. We used special SIMS bulk analysis techniques to measure the impurities in the materials that we used on the program, and found impurities other than those quoted as the dopants (Si, S, SN, Zn, etc.).



Accession For	
NTIS GPA&I	<input checked="checked" type="checkbox"/>
DTIC TAB	<input type="checkbox"/>
Unannounced	<input type="checkbox"/>
Justification	
By _____	
Distribution/	
Availability Codes	
Dist	Special
A-1	

UNCLASSIFIED

SECURITY CLASSIFICATION OF THIS PAGE(When Data Entered)

## EXECUTIVE SUMMARY

We implanted H, He, and most dopant elements into GaAs, GaAsP, GaP, GaSb, InP, InAs, InSb, and LiNbO<sub>3</sub> at energies from 10 to 700 keV, and a few elements up to 2.4 MeV, in random and channeling orientations, annealed some of these implants, and measured their depth distributions using secondary ion mass spectrometry (SIMS). We calculated values of  $R_m$ ,  $R_p$ ,  $\Delta R_p$ ,  $\gamma_1$ ,  $\beta_2$ , using an LSS formulation, and using TRIM (for a few), a Monte Carlo calculation, and measured these same profile parameters for the experimental profiles using a Pearson IV computer fitting routine.

This work included studies of: characterization of Si implantation into GaAs in random and channeling orientations at energies from 10 keV to 6.0 MeV; a general description of as-implanted and annealed depth profiles of dopant implants (especially Be and Si) into GaP, GaAs, InP, and InSb; illustrations of the effects of heterostructures, including superlattices, on the redistribution of mobile impurities (H and Be) during thermal processing; brief illustrations of implants in other III-V technologies (GaAs/Si and GaAsP); lanthanide rare earth elements in III-V crystals; as-implanted and annealed MeV implants in III-V materials; characterization of proton exchanged LiNbO<sub>3</sub>; and redistribution of implanted H in LiNbO<sub>3</sub>.

A significant result of this effort was the establishment of secondary ion mass spectrometry (SIMS) technologies for these materials. The use of our implants of known isotope and fluence provided calibration standards for the quantification of SIMS. We established SIMS relative sensitivity factors for both oxygen and cesium primary ion beams and positive and negative secondary ion mass spectrometry, using the variety of ions implanted. Another significant result of this research program was the measurement of range-energy and range straggle-energy tables and curves for the ions and materials studied. We used special SIMS bulk analysis techniques to measure the impurities in the materials that we used on the program, and found impurities other than those quoted as the dopants (Si, S, Sn, Zn, etc.).

#### ACKNOWLEDGEMENTS

A number of collaborators contributed to the work summarized here, via various publications and measurements. We especially acknowledge D. Jamba, J. Zavada, S. Pearton, S. Novak and the SIMS staff at CHARLES EVANS & ASSOCIATES, D. Ingram, P. Pronko, P. Thompson, R. Laidig and J. Comas

## TABLE OF CONTENTS

Report Documentation Page .....	i
Executive Summary .....	iii
Acknowledgements .....	iv
Table of Contents .....	v
List of Figures .....	vi
I. INTRODUCTION AND STATEMENT OF PROBLEM STUDIED .....	1
II. SUMMARY OF THE MOST IMPORTANT RESULTS .....	2
III. LIST OF ALL PUBLICATIONS .....	3
IV. LIST OF ALL PARTICIPATING SCIENTIFIC PERSONNEL .....	5
V. RESEARCH EFFORT	
A. Communication .....	6
B. Contract Business .....	6
C. Samples Sent to Other Researchers for Measurements, and Type of Measurement .....	6
D. Special Effort-Impurity Analysis in Spectrum Technology GaAs ..	7
E. Si Implanted into GaAs .....	7
F. Implants into III-V Materials .....	7
G. Heterostructures and Interfaces .....	8
H. Other II-V Material Technologies .....	8
I. Rare Earth Implants into II-V Materials .....	9
J. H in II-V Materials .....	9
K. LiNbO <sub>3</sub> .....	9
L. MeV Implants .....	9
M. Other Efforts .....	10
Figures .....	11
Appendix	
A. Summary of work performed related to contract effort .....	18
1. Summary of hydrogen ( <sup>1</sup> H and <sup>2</sup> H, He, Be, Si and other implants into various substrates made for and during the ARO Contract .....	19
2. Summary of implants by material .....	23
3. Summary of annealing temperatures .....	24
4. Summary of implant/annealing/SIMS profiling studies by implant/sample number .....	25

## LIST OF FIGURES

Figure 1.	Be implant compensation of Si channel tail .....	11
Figure 2.	Si depth profiles in GaAs: 4-MeV random $2.5 \times 10^{15}$ Si .....	11
Figure 3.	Si depth profile in GaAs: 6-MeV $\langle 110 \rangle$ channeled $1 \times 10^{15}$ Si .....	11
Figure 4.	Range and range straggle for Si in GaAs .....	11
Figure 5.	Low fluence profiles of Be in GaP and InP .....	12
Figure 6.	Moderate fluence profiles of Be in GaP and InP .....	12
Figure 7.	Annealed profiles of Be in GaP .....	12
Figure 8.	Annealed profiles of Be in InP .....	12
Figure 9.	Annealed profiles of Be in GaAs .....	13
Figure 10.	Channeled profiles of Be in GaP .....	13
Figure 11.	Channeled profiles of Si in GaP .....	13
Figure 12.	Random profiles of Be in InP .....	13
Figure 13.	Channeled profiles of Be in InP .....	14
Figure 14.	Channeled profiles of Si in InP .....	14
Figure 15.	Channeled profiles of Be in InSb .....	14
Figure 16.	Channeled profiles of Si in InP .....	14
Figure 17.	Annealed channeled profile of Be in InP .....	15
Figure 18.	Redistribution of H in GaAs .....	15
Figure 19.	Furnace vs Flash lamp annealing for H in GaP .....	15
Figure 20.	Layers in an AlAs/GaAs superlattice .....	15
Figure 21.	H redistribution in an AlAs/GaAs superlattice .....	16
Figure 22.	Redistribution of H in an superlattice/buffer .....	16
Figure 23.	Redistribution of Be in an superlattice .....	16
Figure 24.	Redistribution of H in a GaAs/Si structure .....	16
Figure 25.	Random depth profile of Sm implanted into GaAs .....	17
Figure 26.	Channeled depth profile of Sm implanted into GaAs .....	17
Figure 27.	Depth profiles of MeV Si in GaAs, GaP, InP, and InSb .....	17
Figure 28.	Depth profiles of 0.7 MeV Be in InP .....	17

## I. INTRODUCTION AND STATEMENT OF PROBLEM STUDIED

The objectives of this program were to provide understanding for the Army and DoD of III-V semiconductor materials and devices that can be fabricated in these materials as a result of the energy deposition or momentum transfer of energetic light ions via alteration of the properties of the materials. Affected properties include changes of the index of refraction, diffusion coefficients, or electrical characteristics (e.g., by defects, vacancies, scattering centers, etc.), as well as direct effects of changes in the electrical (semiconducting) properties of the crystalline material caused by the presence of the implanted atoms as n- or p-type dopants (donors or acceptors). In addition, information was needed about changes of all of the above effects caused by thermal processing of either short (seconds) or long (minutes) duration. These III-V materials were single crystals of one material or combined material structures (heterostructures), for example, superlattices.

The pursuit of these general objectives entails the implantation of elements as ions from throughout the periodic table, but because of the focus on III-V materials and waveguide applications, we were primarily concerned with the light ions  $^1\text{H}$ ,  $^2\text{H}$ , and  $^4\text{He}$ , and those from columns II, IV, and VI of the periodic table, especially Be, Mg, Ca, Zn, Sr, Cd, C, Si, Ge, Sn, O, S, Se, and Te. The ion energy range of interest was large because of the varied applications, including wave guiding structures in the infrared (tens of  $\mu\text{m}$ ) and deep and shallow device structures (0.1 to 1.0  $\mu\text{m}$ ).

To meet these goals, we first obtained polished wafers of four III-V materials, GaP, GaAs, InP, and InSb, from a variety of sources. These materials were obtained both undoped and highly n-doped ( $>10^{18} \text{ cm}^{-3}$ ), the latter for waveguide fabrication via carrier removal. Crystals having the commonly available orientations (100) and (111), as well as (110) when possible, were obtained for channeling studies, an alternative method to MeV implantation to achieve deep penetration. During the course of this program, we received samples of InAs and GaSb from S. Pearton of ATT Bell Labs, for which we are grateful. We implanted the ions listed above at energies between 50 and 2000 keV in random and channeling orientations (the latter by aligning the desired crystal direction using Rutherford backscattering), at fluences between  $5 \times 10^{12}$  and  $10^{14} \text{ cm}^{-2}$ , or higher fluences for the light ions  $^1\text{H}$ ,  $^2\text{H}$ , and  $^4\text{He}$ , as appropriate for waveguide fabrication by carrier removal, namely,  $10^{15}$  to  $10^{16} \text{ cm}^{-2}$ . We then annealed selected samples using furnace or rapid lamp annealing at temperatures appropriate for each material. The melting temperatures for GaSb and InSb are so low that little annealing effect could be achieved. GaP can withstand the highest temperatures. However, annealing temperatures were limited to 800°C for all materials using furnace annealing, and to 900°C using rapid lamp annealing.

## II. SUMMARY OF THE MOST IMPORTANT RESULTS

We implanted H, He, and most dopant elements into GaAs, GaAsP, GaP, GaSb, InP, InAs, InSb, and LiNbO<sub>3</sub> at energies from 10 to 700 keV, and a few elements up to 2.4 MeV, in random and channeling orientations, annealed some of these implants, and measured their depth distributions using secondary ion mass spectrometry (SIMS). We calculated values of  $R_m$ ,  $R_p$ ,  $\Delta R_p$ ,  $\gamma_1$ ,  $\beta_2$ , using an LSS formulation, and using TRIM (for a few), a Monte Carlo calculation, and measured these same profile parameters for the experimental profiles using a Pearson IV computer fitting routine.

This work included studies of: characterization of Si implantation into GaAs in random and channeling orientations at energies from 10 keV to 6.0 MeV; a general description of as-implanted and annealed depth profiles of dopant implants (especially Be and Si) into GaP, GaAs, InP, and InSb; illustrations of the effects of heterostructures, including superlattices, on the redistribution of mobile impurities (H and Be) during thermal processing; brief illustrations of implants in other III-V technologies (GaAs/Si and GaAsP); lanthanide rare earth elements in III-V crystals; as-implanted and annealed MeV implants in III-V materials; characterization of proton exchanged LiNbO<sub>3</sub>; and redistribution of implanted H in LiNbO<sub>3</sub>.

A significant result of this effort was the establishment of secondary ion mass spectrometry (SIMS) technologies for these materials. The use of our implants of known isotope and fluence provided calibration standards for the quantification of SIMS. We established SIMS relative sensitivity factors for both oxygen and cesium primary ion beams and positive and negative secondary ion mass spectrometry, using the variety of ions implanted. Another significant result of this research program was the measurement of range-energy and range straggle-energy tables and curves for the ions and materials studied. We used special SIMS bulk analysis techniques to measure the impurities in the materials that we used on the program, and found impurities other than those quoted as the dopants (Si, S, Sn, Zn, etc.).

### III. LIST OF ALL PUBLICATIONS

Publications: Publications and conference presentations that resulted from this program are listed below.

1. J.M. Zavada, H.A. Jenkinson, R.G. Sarkis, and R.G. Wilson, "Hydrogen depth profiles and optical characterization of annealed, proton implanted n-type GaAs," J. Appl. Phys. 58, 3731-3734 (1985)
2. R.G. Wilson, "Implant profiles in GaP, GaAs, InP, and InSb: influence of furnace and rapid thermal annealing," Proc. SPIE .... FLA 1987
3. P.E. Thompson, R.G. Wilson, D.C. Ingram, and P.P. Pronko, "Atomic profiles of high energy (MeV) Si implanted into GaAs," Mat. Res. Soc. Proc. 93, 73-77 (1987)
4. J.M. Zavada, R.G. Wilson, and S.W. Novak, "Accumulation of implanted hydrogen at the superlattice/substrate interface of a GaAs-AlAs multilayer structure," EESDERC Bologna, Italy, Sept, 1987
5. J.M. Zavada, R.G. Wilson, S.W. Novak, A.R. von Neida, and S.T. Pearton, "Redistribution of implanted hydrogen in p<sup>+</sup> GaAs(Zn) and n<sup>+</sup> GaAs(Si) single crystals," Proc. MRS Boston, Dec 1987
6. S.W. Novak and R.G. Wilson, "SIMS measurements of impurities and dopants in AlGaAs heterostructures," Proceedings of the Sixth International Conference on Secondary Ion Mass Spectrometry (SIMS VI), Versailles, France, September 1987, pp. 303-06
7. R.G. Wilson, S.W. Novak, and J.M. Zavada, "Redistribution of implanted hydrogen and substrate dopants in annealed (100 to 600 °C) substrates of GaP(S), InP(S), InP(Sn), GaAs(Si), and GaAs(Zn)," Inst. Phys. Conf. Ser. 91, 475-77 (1987)
8. R.G. Wilson, S.W. Novak, and J.M. Zavada, "Depth distributions of Be and Si implanted into GaP, InP, and InSb, after implantation and after furnace or flash lamp annealing, compared with GaAs," Inst. Phys. Conf. Ser. 91, 479-83 (1987)
9. R.G. Wilson, J.M. Zavada, S.W. Novak, and S.P. Smith, "Depth profiles and redistribution during annealing of 300-keV hydrogen (protons) implanted into an AlAs/GaAs superlattice," Inst. Phys. Conf. Ser. 91, 485-88 (1987)
10. S.W. Novak and R.G. Wilson, "Two- and three-dimensional characterization of AlGaAs heterostructures using SIMS," Inst. Phys. Conf. Ser. 91, 597-600 (1987)
11. R.G. Wilson, D.M. Jamba, D.C. Ingram, P.P. Pronko, P.E. Thompson, and S.W. Novak, "Ranges, straggles, and shape factors of 20-keV through 6 MeV random and channeled Si implants into GaAs, unannealed and annealed," Inst. Phys. Conf. Ser. 91, 809-12 (1987)
12. J.M. Zavada, R.G. Wilson, and J. Comas, "Redistribution of H and Be in GaAs/AlAs multilayer structures with post implantation annealing," J. Appl. Phys. 65, 1968-71 (1989)
13. R.G. Wilson and D.B. Rensch, "Implantation and characterization of III-V materials," (Invited) Annual Materials Research Society Meeting, Sept., 1987, Boston, MA, J. Materials Research Society Vol. , page (1989)
14. J.M. Zavada, R.G. Wilson, and J. Comas, "Ion beam processing of multilayer semiconductor structures, SPIE Symp. on Laser Technology in Industry, Porto, Portugal, 6-8 June 1988
15. J.M. Zavada, S.J. Pearton, R.G. Wilson, C.S. Wu, M. Stavola, F. Ren, J. Lopata, W.C. Dautremont-Smith, and S.W. Novak, "Electrical effects of atomic hydrogen incorporation in GaAs-on-Si," J. Appl. Phys. 65, 347-53 (1989)

16. R.G. Wilson, "Implantation range statistics in III-V materials," (Invited) ECS Conference on Ion Implantation in Compound Semiconductors, Hollywood, FL, 16-20 Oct 1989. To be published in the ECS Conference Proceedings.
17. R.G. Wilson, J.M. Zavada, and S.W. Novak, "As-implanted and annealing behavior of 0.20, 0.35, and 1.0 MeV  $^1\text{H}$  and  $^2\text{H}$  implants into InP, and comparison with GaAs," (Invited) Workshop on Hydrogen Effects in InP and Related Compounds, Lannion, France, 24-25 October 1989
18. R.G. Wilson, S.W. Novak, J.M. Zavada, A. Loni, and R.M. De La Rue, "SIMS depth profiling of proton-exchanged  $\text{LiNbO}_3$ ," J. Appl. Phys. 15 Dec, xxx (1989)
19. R.G. Wilson, S.W. Novak, J.M. Zavada, A. Loni, and R.M. De La Rue, "SIMS of  $\text{H:LiNbO}_3$ ," Secondary Ion Mass-Spectrometry SIMS VII, H. Storms, ,Eds. [Wiley, NY, 1990] pp. xxx-xxx (Monterey, CA, Sept 1989) (to be published soon)
20. A manuscript has been prepared for submission to J. Appl. Phys., titled "Systematics of SIMS relative sensitivity factors versus electron affinity and ionization potential for a variety of matrices determined from implanted calibration standards for about fifty elements," by R.G. Wilson and S.W. Novak, that acknowledges ARO support for the work in III-V materials.

IV. LIST OF ALL PARTICIPATING SCIENTIFIC PERSONNEL

DEGREES AWARDED DURING THIS REPORTING PERIOD:

None

SCIENTIFIC PERSONNEL SUPPORTED BY THIS PROJECT:

CHARLES EVANS & ASSOCIATES

Scott M. Baumann  
Richard J. Blattner  
Dr. Roger J. Bleiler  
Dr. Paul K. Chu  
Daniel Cudworth  
Ramon DeSantiago  
Dr. Charles A. Evans, Jr.  
Charles J. Hitzman  
Craig G. Hopkins  
Igor Ivanov  
Dr. Clive M. Jones  
Donald Martin  
Dr. Charles Kirschbaum  
Dr. Gayle Lux  
Dr. Steven W. Novak  
James C. Norberg  
Dr. Steven S. Smith  
Elizabeth M. Strathman  
Shaun D. Wilson

HUGHES RESEARCH LABORATORIES

Dr. Robert G. Wilson

## V. RESEARCH EFFORT

### Communication:

Communication between R. Wilson in California and J. Zavada in London regarding this contract program was carried out via many phone calls, FAX transmissions, and data packages mailed via the New York APO address during 1986, 1987, 1988, and 1989.

Wilson met with M. Littlejohn at the International Symposium on GaAs and Related Compounds in Hraklion, Crete, during September, 1987, where they discussed results and plans for future work. Wilson met with Littlejohn in Malibu, CA, during March of 1988 to discuss progress and future plans for work on this contract.

Wilson and Zavada met in Mailbu, CA, during December of 1987 and December of 1988 to discuss detailed technical work, to review progress, and to plan future work on this contract effort. Wilson met with Zavada once in London in Apr 1987, and once in France at the H in InP Workshop in Oct 1989 to discuss in detail technical work for this contract.

Wilson visited Charles Evans and Associates in Redwood City, CA almost once each month during the more than three years duration of the program, where he and staff members of Evans and Associates discussed work to be done and work completed, and worked together to carry out many SIMS analyses on samples prepared for the contract. S.W. Novak was the primary Evans and Associates staff member involved in this interaction and contributed greatly to the work and results of this effort.

Contract Business: A no cost time extension was requested and granted for this program. The modified contract ending date was 30 Oct 1989, with the final report due 60 days after that. This modified date included the time of the ERO/ARO sponsored H:InP workshop in Lannion, France, at which an invited paper was presented on work performed on this contract.

### Samples Sent to Other Researchers for Measurements, and Type of Measurement

The following implants were performed and mailed to H. Jenkinson at Picatinny Arsenal for carrier removal/optical measurements:

He 152	250 keV	1.0E14 cm <sup>-2</sup>	into InP(Sn)	
He 153	250 keV	1.0E14 cm <sup>-2</sup>	into InP(S)	
He 154	250 keV	1.0E14 cm <sup>-2</sup>	into InP(Zn)	
D 227	300 keV	5.0E15 cm <sup>-2</sup>	into GaAs(Zn) + 100, 200, 300, 400, 500, 600°C Anneals	
D 230	100 keV	5.0E15 cm <sup>-2</sup>	into GaAs/Si epi	
H 3590	100 keV	1.0E16 cm <sup>-2</sup>	into LiNbO <sub>3</sub>	
D 282	100 keV	1.0E16 cm <sup>-2</sup>	into LiNbO <sub>3</sub>	

Samples sent to other workers:

H3519	300 keV	1.0E16 cm <sup>-2</sup>	+ GaAs(Zn)	to S. Pearton ATT	electrical
H3534	50 keV	5.0E15 cm <sup>-2</sup>	+ NRL SL 711	to G. Hubler NRL	optical
			+ 300, 500°C Anneals		

2 Be, 3 Zn, 4 Si, & Se as-  
implanted and annealed -  
most 200 keV,  $1.0 \times 10^{14} \text{ cm}^{-2}$

to Prof. Henry Lozykowski  
Dept. Electr. & Computer Engr.  
Ohio Univ. Athens, OH 45701  
(614) 593-1587

optical  
electr.

### Special Effort - Impurity Analysis in Spectrum Technology GaAs

An impurity analysis was performed using SIMS on four pieces of bulk LEC GaAs grown by Spectrum Technology. This effort was requested by M. Littlejohn, for ARO. Pieces from seed and tang of two boules were studied (ST 045, 053, 121, and 157). The impurities analyzed were B, C, O, Na, Mg, Si, S, Cr, Mn, Fe, Cu, Zn, Se, In, and Te. Several other pieces of LEC GaAs and one piece of HB GaAs were analyzed at the same time. The results for the ST material were comparable with other material and no impurity was unusually high. B was higher than for HB material but comparable with other LEC material that was also grown in a pBN crucible.

### Si Implanted into GaAs

We implanted Si into GaAs at energies from 10 keV to 6.0 MeV in random and  $\langle 110 \rangle$  channeling orientations, annealed some of these implants with proximity caps at 750 or 800°C for 15 or 20 min in a furnace, or for 10 or 15 s in a flash lamp annealer, and measured atom depth distributions using SIMS and some electrical profiles using C-V [3,8,11]. Conclusions from this work include: Si atoms do not redistribute during furnace anneals up to 800°C or during flash lamp anneals up to 1000°C, for fluences from  $10^{12}$  to  $10^{14} \text{ cm}^{-2}$ ; maximum Si density in  $\langle 110 \rangle$  channeled regions is  $2 \times 10^{16} \text{ cm}^{-3}$ ;  $\langle 110 \rangle$  channeled depths are about  $1 \mu\text{m}$  at 20 or 40 keV and up to  $12 \mu\text{m}$  at 6 MeV; SIMS detection sensitivity for  $^{30}\text{Si}$  in GaAs is about  $1 \times 10^{14} \text{ cm}^{-3}$  ( $3 \times \text{BG}$ ); experimental ranges ( $R_p$ ) are 0 to 20% deeper than LSS calculations, and experimental range straggles ( $\Delta R_p$ ) are about 50% greater than LSS calculations at lower energies, but approach the same values as energy increases, until they converge at a few MeV;  $\langle 110 \rangle$  channeled profile shape varies with ion energy, having three peaks at 6 MeV and relatively constant Si density from 3 to  $11 \mu\text{m}$ . Random and channeled MeV Si implants are illustrated in Figs. 2 and 3. Random and channeled range and range straggles are illustrated vs energy in Fig. 4; note the changes in slope at about 1 MeV.  $R_c$  is the depth of the channeled peak in the profile and  $R_{\text{max}}$  is the maximum range of the channeled ions. Figure 1 shows how Be or g can be used to compensate the deep tail on Si implants to sharpen the n-type profile and improve the electrical characteristics of FETs -- taken from publication 13, but this device portion of the work was not funded by ARO.

### Implants into III-V Materials

We implanted the elements Be, Mg, Zn, Cd, C, Si, Ge, Sn, O, S, Se, Te,  $^1\text{H}$ , and  $^2\text{H}$  into GaS, GaP, and InP, and some of them into GaSb, InSb, and InAs, and annealed the more commonly used combinations with proximity caps in a furnace or flash lamp annealer [7,8]. Most elements were also channeled into the  $\langle 110 \rangle$  direction of GaAs and InP, and the  $\langle 111 \rangle$  or  $\langle 100 \rangle$  direction of GaP. We measured their depth distributions using  $\text{O}_2$  or Cs

SIMS, and in some cases, using C-V. We calculated  $R_m$ ,  $R_p$  ( $\mu$ ),  $\Delta R_p$  ( $\sigma$ ),  $\gamma_1$ , and  $\beta_2$  using an LSS formulation, and determined the corresponding experimental values using a Pearson IV computer fitting routine. The agreement is only fair because the LSS formulation assumes amorphous targets and the experimental data are for crystalline material; the agreement becomes much better when crystalline targets are pre-amorphized by self implants.

For SIMS, we measured the relative sensitivity factors (RSF) for quantification, the detection limits or sensitivities, the profile dynamic range, and molecular ion intensity comparisons. Various illustrations of the results are shown in Figs. 5 through 17. Conclusions from this work include: for normal implant conditions (channel or source/drain and 800°C), Be redistributes most in InP, less in GaAs, and little or not at all in GaP; Mg is similar to Be; Si does not redistribute in any III-V material, Ge is similar to Si, for fewer cases studied; and Sn diffuses in GaAs and possibly in other materials. The depth profile of associated damage in these implants is an issue, but is not dealt with here because of the difficulty of experimental measurement. Redistribution of implanted H into III-V materials is illustrated in Fig. 18 for GaAs. The H migrates deeper into the bulk at a density of about  $3 \times 10^{18} \text{ cm}^{-3}$  with a strong temperature dependence, much as for thermal diffusion, but probably also depending on the diffusion and annihilation of defects. A comparison of the effects of furnace and flash lamp annealing is illustrated in Fig. 19 for GaP. Similar results were observed for GaAs and InP.

### Heterostructures and Interfaces

We implanted several heterostructures and superlattices and profiled both the matrix and impurity using SIMS [9,10]. An example is shown in Figs. 20 and 21, where an AlAs/GaAs structure implanted with H is shown via the Al depth profile (Fig. 20), which is disordered and collapses for a 500°C thermal treatment. The implanted H redistributes to the interface between the superlattice and the GaAs substrate as shown in Fig. 21, where it still remains after a 700°C thermal treatment. Similar superlattices are shown in Figs. 22 and 23, but grown on a GaAs buffer layer, and implanted with both H and Be. Here, both the H and Be redistribute to the buffer/substrate interface. However, the Be redistributes less and only significantly for a temperature of 600°C.

### Other III-V Materials Technologies

We implanted Si-doped GaAs on Si (MBE) epi wafers with H and profiled the Si and H as a function of annealing temperature to 700°C [15]. The Si profile is unchanged and the H redistributes to the GaAs/Si interface where it remains greater than  $10^{20} \text{ cm}^{-3}$  even for the 700°C anneal, indicating that the strain (or defects at the interface) remains after this anneal temperature. These results are illustrated in Fig. 24. We implanted GaAsP with a variety of dopants and other elements and profiled them using SIMS. The results are similar to those for GaP and GaAs.

### Rare Earth Implants into III-V Materials

We implanted many of the rare earth elements (Sc, Y, La, Ce, Nd, Sm, Eu, Tb, Dy, Ho, Er, Tm, Yb) into GaAs and InP in random and  $\langle 110 \rangle$  channeling orientations and profiled them using SIMS. There is some interest in doping InP-based materials with these materials, esp. Er. The results confirm that these elements can be implanted in our standard implanter and that the depth profiles are consistent with those of surrounding elements. Random ranges are 70 to 90  $\mu\text{m}$  for 300 keV.  $\langle 110 \rangle$  channelled ranges are 2 to 3  $\mu\text{m}$  for 300 keV. Maximum  $\langle 110 \rangle$  channelled densities are about  $3 \times 10^{15} \text{ cm}^{-3}$ . Examples of random and channelled profiles are shown in Figs. 25 and 26, respectively, for Sm in GaAs.

### H in III-V Materials

$^2\text{H}$  shows the redistribution of H in III-V materials better than  $^1\text{H}$  because of the 100x better detection capability of SIMS for  $^2\text{H}$ .

III-V materials doped with H using plasmas or ion implantation plus anneals result in the same depth distributions.

H concentration is  $\sim 100\text{x}$  higher in p-type (Zn-doped) III-Vs than in n-type (S-, Si-, or Sn-doped) III-Vs.

### LiNbO<sub>3</sub>

LiNbO<sub>3</sub> is another material that is important for wave guides. Work on LiNbO<sub>3</sub> was emphasized during the latter part of this contract, including samples of hydrogen-exchanged LiNbO<sub>3</sub> received from the University of Glasgow. A special SIMS technology was developed to profile this dielectric (charging) material. We also annealed a few representative implants in LiNbO<sub>3</sub> at 600°C/10min to determine the temperature stability of implants in LiNbO<sub>3</sub> under this one condition. The implants selected were H, B, F, P, Cl, Ge, Sb, and Te. Only H showed any redistribution upon annealing at 600°C, and the H redistributed enough that no measurable H depth profile remained.

LiNbO<sub>3</sub> was SIMS profiled at  $\sim 1.0\text{nm/s} \rightarrow 10\mu\text{m/hr} \rightarrow \sim 1\text{K}\$/\text{profile}$

### MeV Implants

The MeV implant phase of this program consisted of implanting high energy H, He, Be, Si, and Ge into various materials, annealing them at various temperatures up to 750°C, and measuring the as-implanted and annealed depth distributions using SIMS.

The following MeV implants were performed:

1.0 MeV	3.0E15	cm <sup>-2</sup>	H
2.0 MeV	5.0E15	cm <sup>-2</sup>	He
0.7 MeV	1.3E13	cm <sup>-2</sup>	Be
2.0 MeV	1.0E14	cm <sup>-2</sup>	Si
2.4 MeV	1.0E14	cm <sup>-2</sup>	Ge

plus 1.0, 2.0, 4.0, and 6.0 MeV Si into GaAs in random and <110> channeling orientations, in collaboration with Universal Energy Systems, and measured also for C-V electrical profiles by Naval Research Laboratory into materials that included GaAs, GaAs(Si), GaP(S), InP(S), InP(Fe), InSb, GaSb(few), and LiNbO<sub>3</sub>. The as-implanted and annealed (750°C/20 min) Be profiles were measured. The as-implanted and annealed (300°C) He profiles were measured. The as-implanted and some annealed (300 and 500°C,) H samples have been profiled. Additional anneal temperatures would be useful if the program is renewed. The 1-MeV H depths are all of the order of 15  $\mu$ m. The ranges of 0.7 MeV Be and 2.0 MeV Si are about 1.6  $\mu$ m. Representative depth profiles are illustrated in Figs. 27 and 28. The annealed profiles are different in the various materials. For example, the H has redistributed very little in the GaP compared with InP and GaAs, which are different from one another as well. The results for annealed Be are similar, namely, Be has not redistributed in GaP, has redistributed in both directions to form a rounded hump in InP, and has formed a non symmetric and structured profile in GaAs.

#### Other Efforts

Work on GaP was emphasized during the latter part of the contract.

Implants of the lanthanide rare earths were also successfully carried out, into GaAs and InP.

Special work was performed on H and D plasma diffused samples of GaAs received from Bell Laboratories.

Samples of GaAsP provided through S.W. Novak of Charles Evans and Associates were implanted, annealed, and profiled using SIMS.

Samples of InAs and GaSb received from Bell Laboratories were implanted with a variety of elements and profiled using SIMS.

# FIGURES

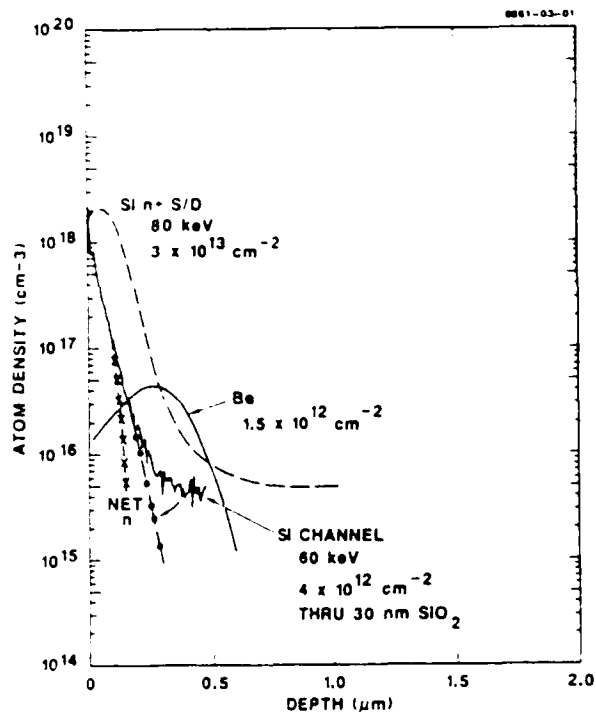


Fig. 1. Be implant compensation of Si channel tail

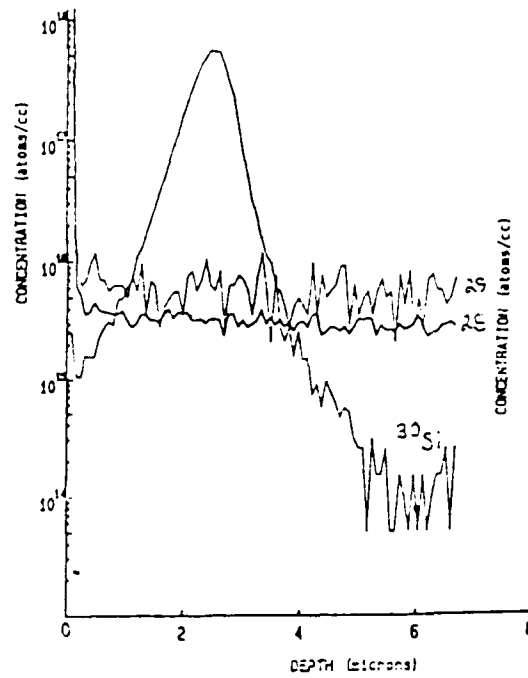


Fig. 2. Si depth profiles in GaAs: 4-MeV random  $^{28,29,30}\text{Si}$

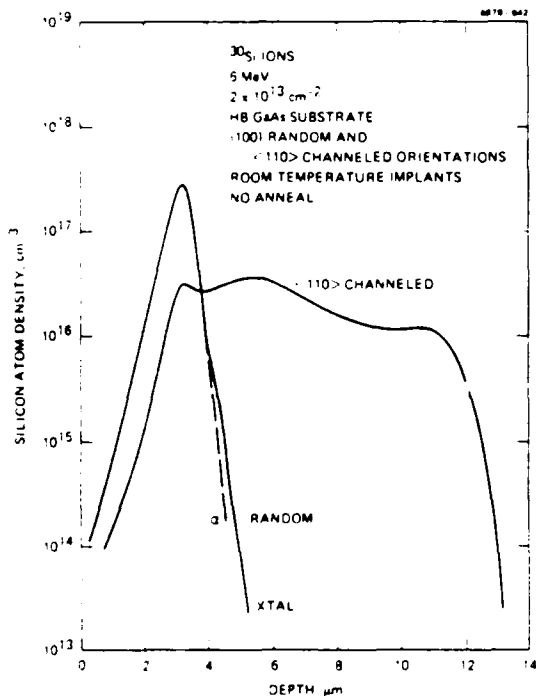


Fig. 3. Si depth profile in GaAs: 6-MeV  $\langle 110 \rangle$  channeled  $^{30}\text{Si}$

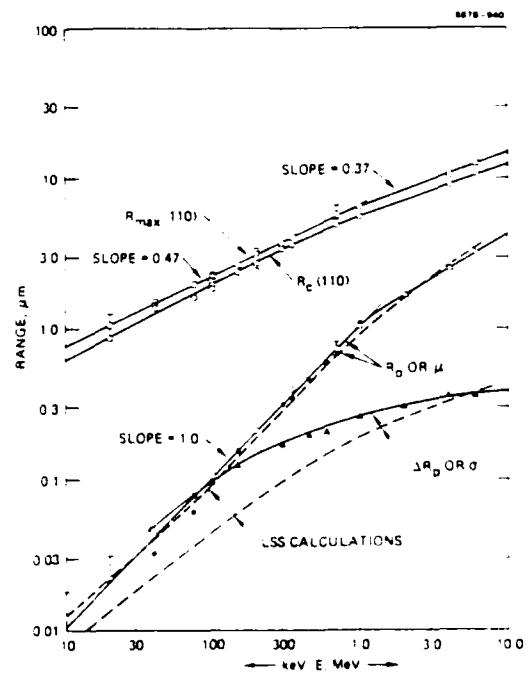


Fig. 4. Range and range straggles for Si in GaAs

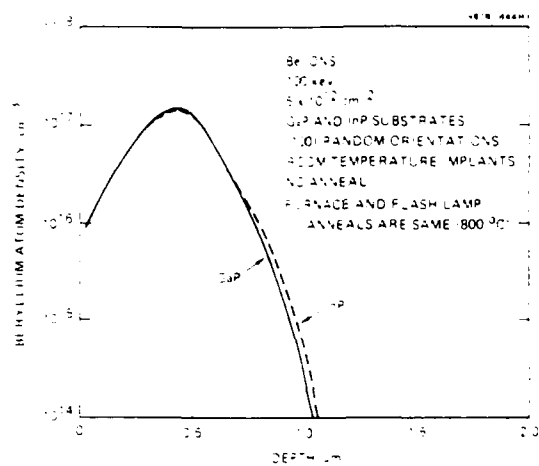


Fig. 5. Low fluence profiles of Be in GaP and InP

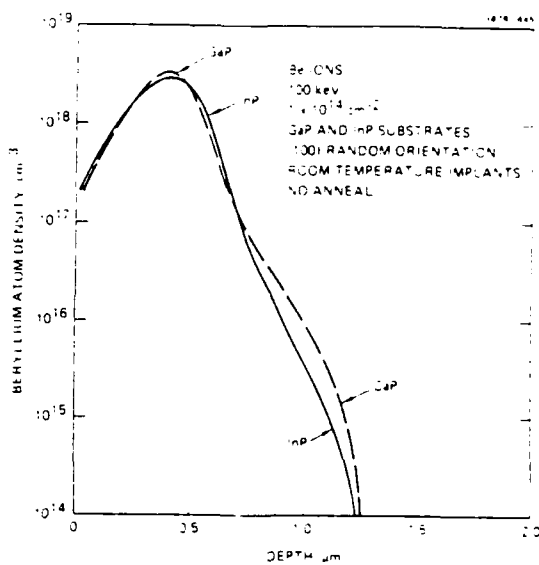


Fig. 6. Moderate fluence profiles of Be in GaP and InP

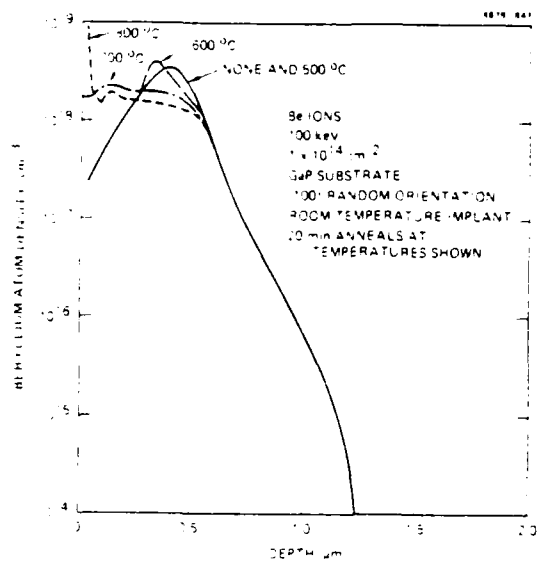


Fig. 7. Annealed profiles of Be in GaP

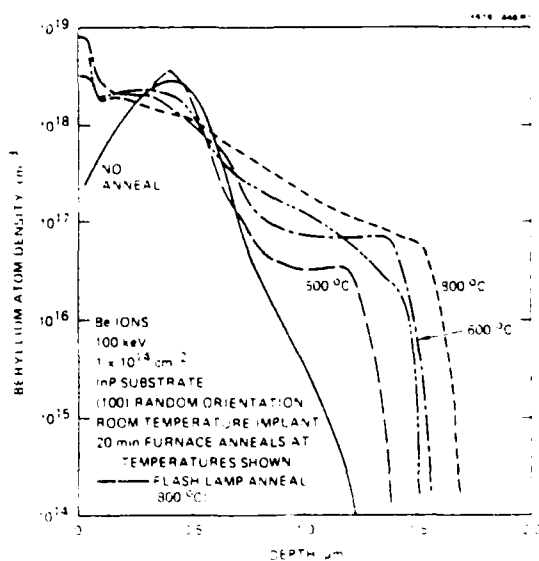


Fig. 8. Annealed profiles of Be in InP

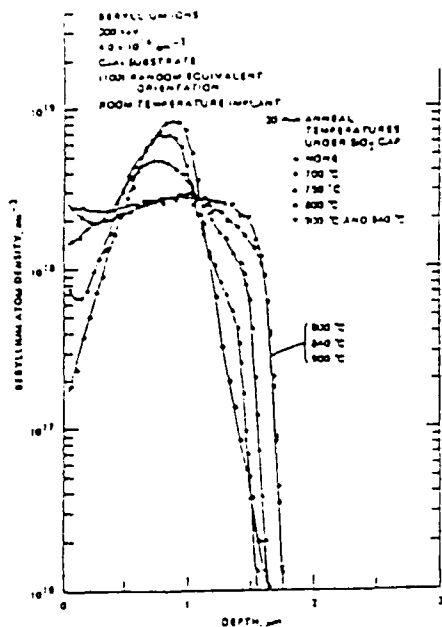


Fig. 9. Annealed profiles of Be in GaAs

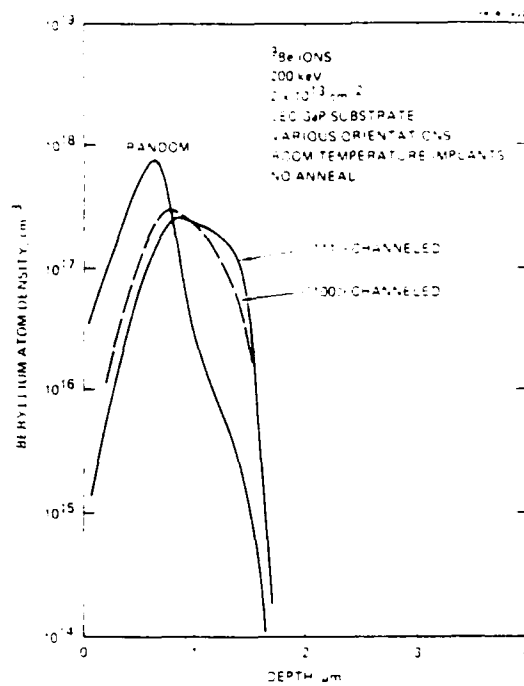


Fig. 10. Channeled profiles of Be in GaP

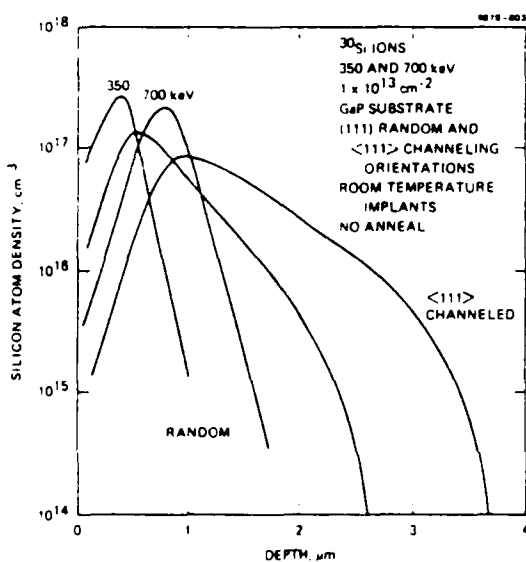


Fig. 11. Channeled profiles of Si in GaP

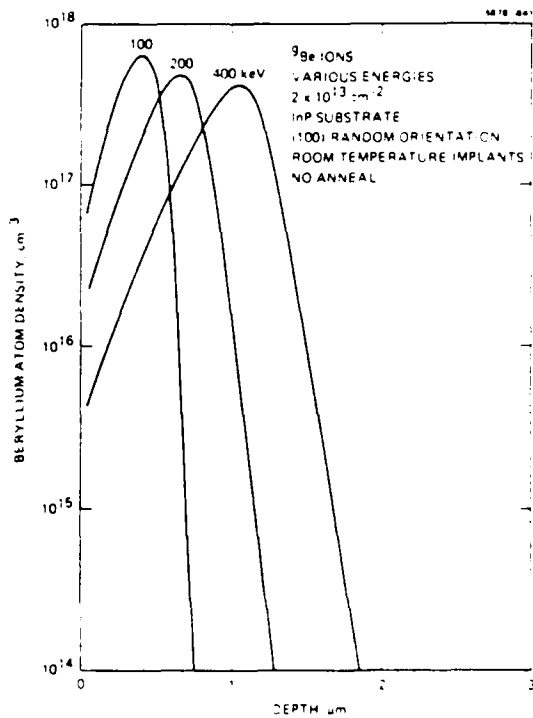


Fig. 12. Random profiles of Be in InP

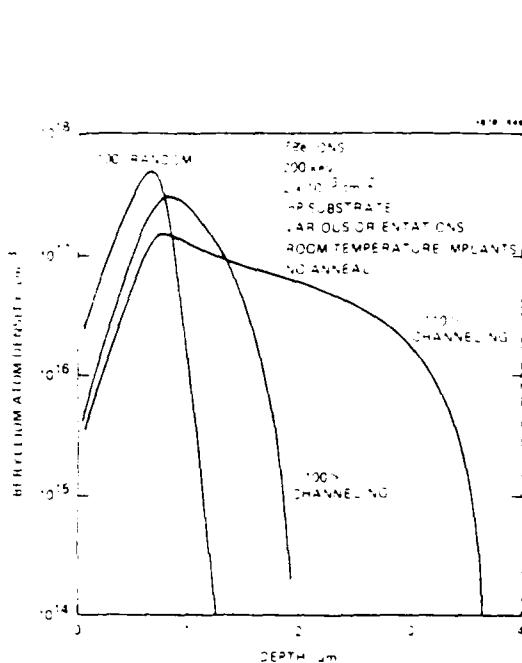


Fig. 13. Channelled profiles of Be in InP

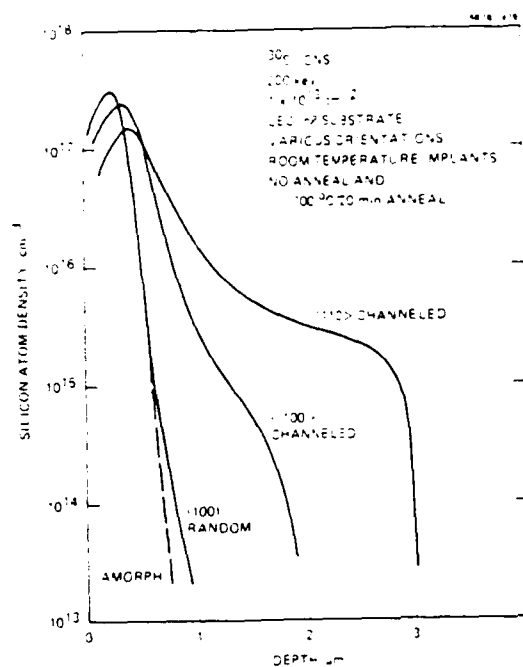


Fig. 14. Channelled profiles of Si in InP

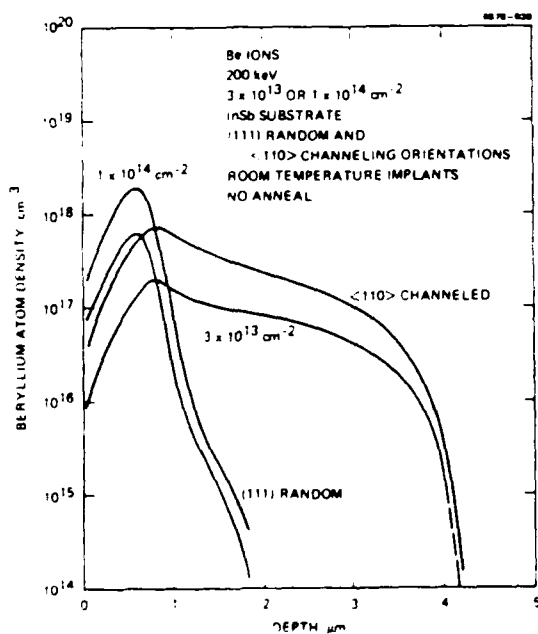


Fig. 15. Channelled profiles of Be in InSb

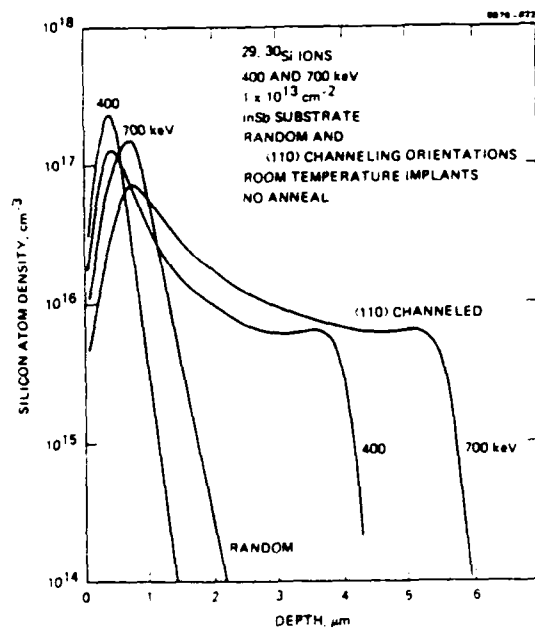


Fig. 16. Channelled profiles of Si in InP

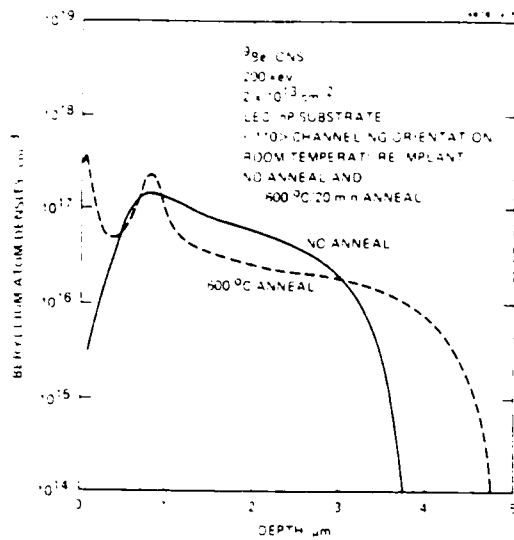


Fig. 17. Annealed channeled profile of Be in InP

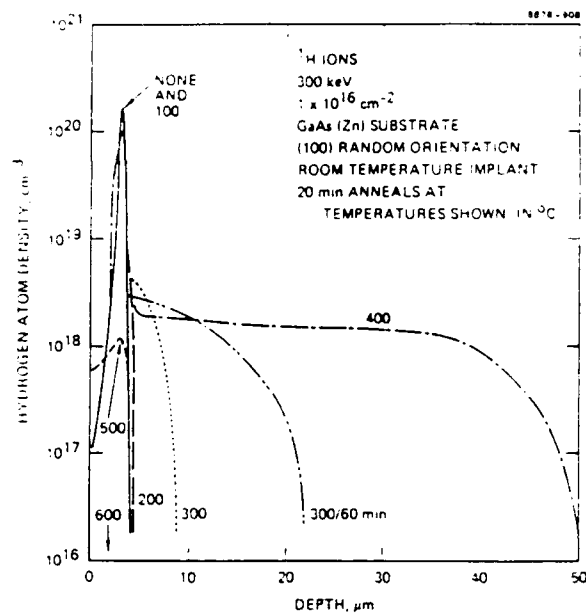


Fig. 18. Redistribution of H in GaAs

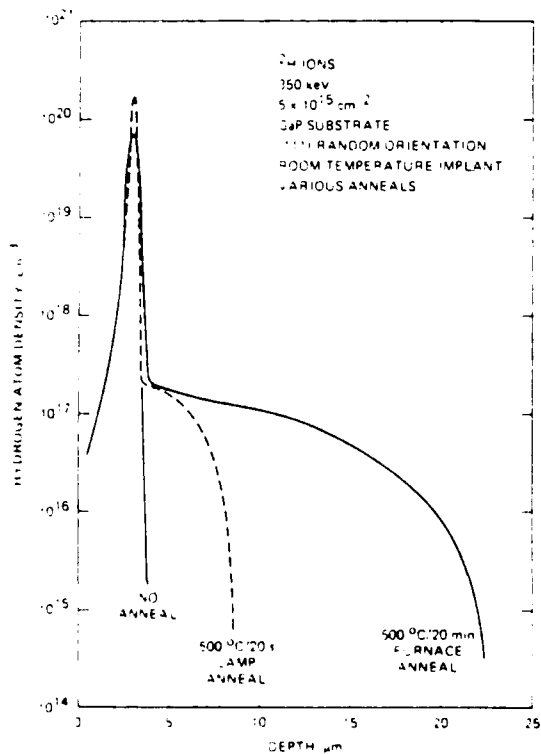


Fig. 19. Furnace vs flash lamp annealing for H in GaP

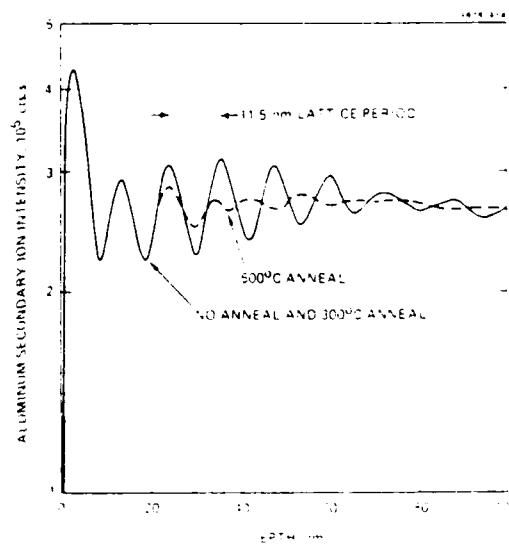


Fig. 20. Layers in an AlAs/GaAs superlattice

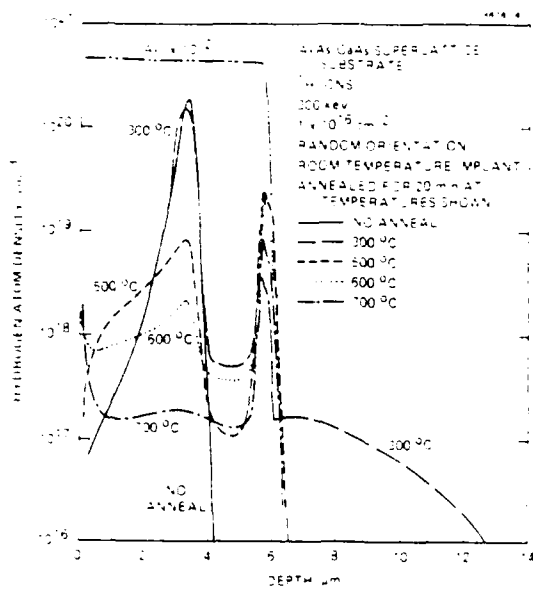


Fig. 21. H redistribution in an AlAs/GaAs superlattice

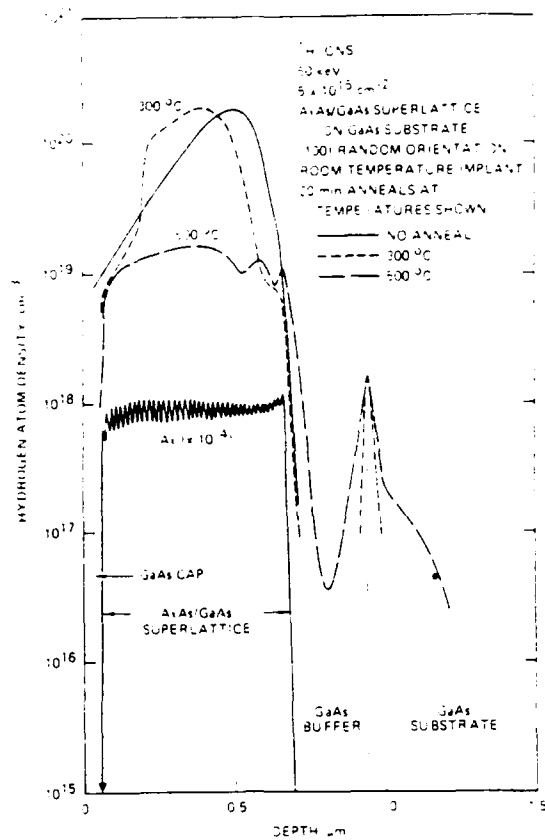


Fig. 22. Redistribution of H in a superlattice/buffer

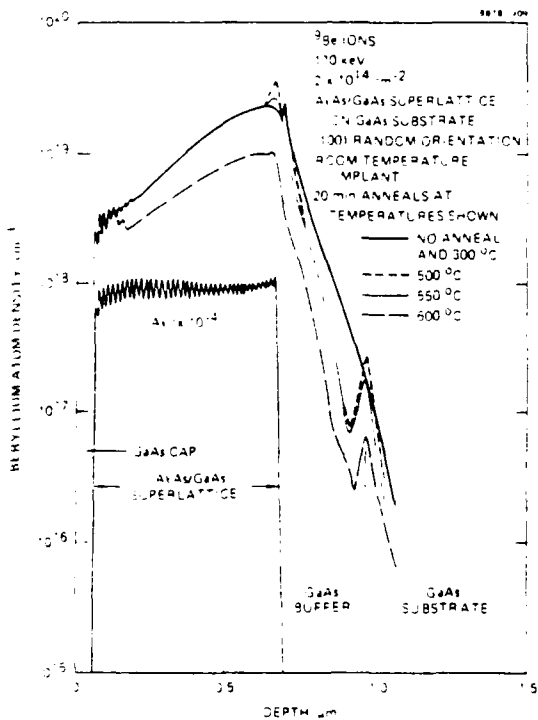


Fig. 23. Redistribution of Be in a superlattice/buffer

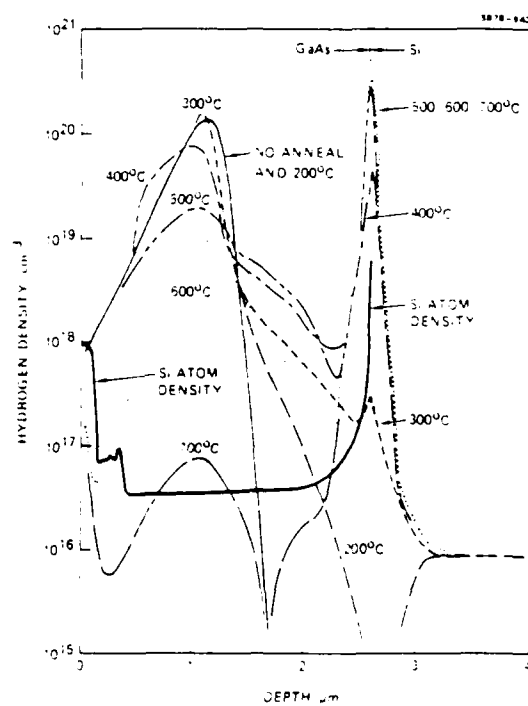


Fig. 24. Redistribution of H in a GaAs/Si structure

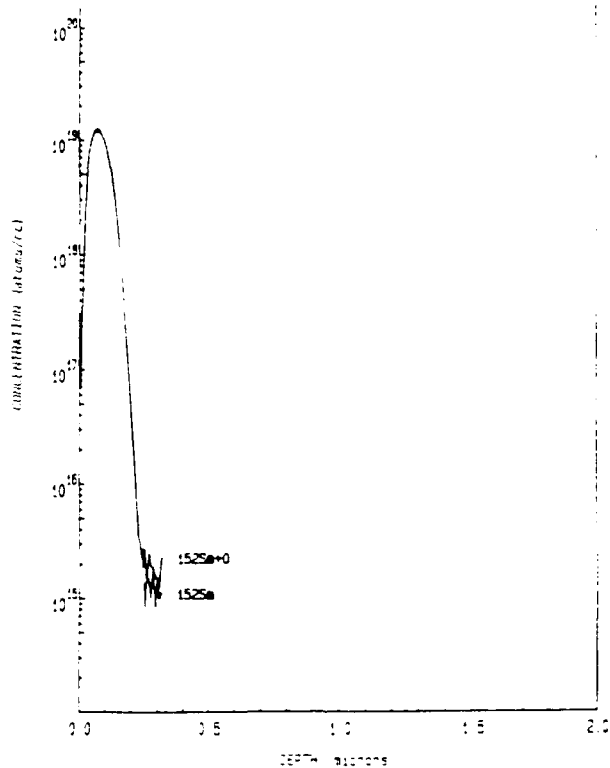


Fig. 25. Random depth profile of Sm implanted into GaAs

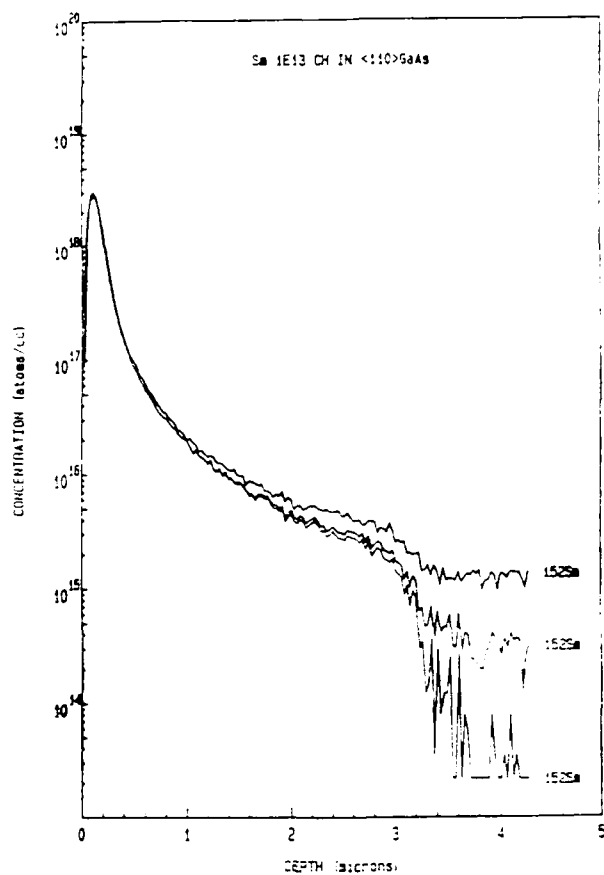


Fig. 26. Channeled depth profile of Sm implanted into GaAs

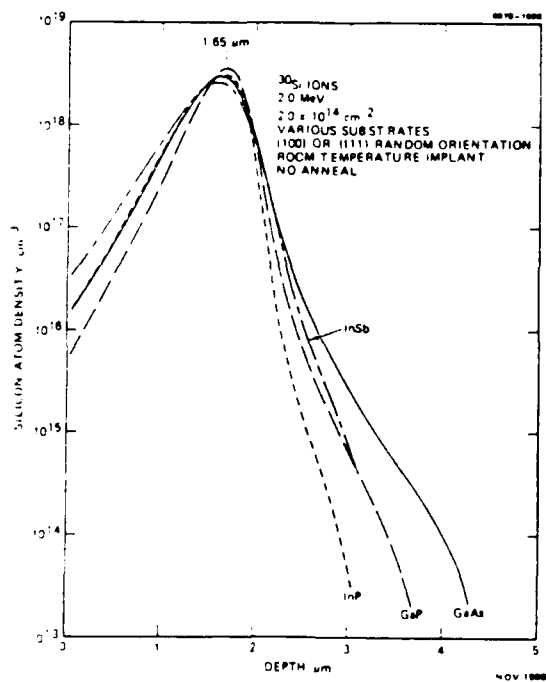


Fig. 27. Depth profiles of MeV Si in GaAs, GaP, InP, and InSb

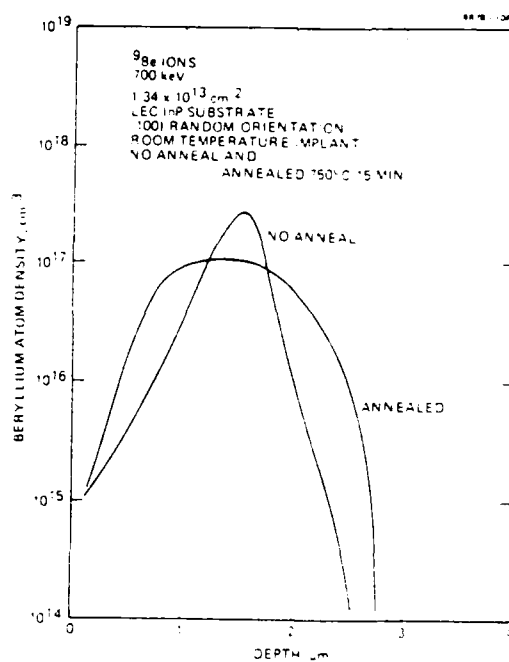


Fig. 28. Depth profiles of 0.7MeV Be in InP

## APPENDIX

On following pages are summary listings of work performed that is related to this contract effort. Included are lists of implants and anneal conditions, by implanted element and by material, a list of anneal temperatures by sample number, and a list of art code numbers by sample number. Finally, brief summaries of measurements made and results obtained are given by sample number, for some, but not all samples.

Summary of Hydrogen [ $^1\text{H}$  and  $^2\text{H}$  (deuterium)], He, Be, Si, and other Implants into Various Substrates (primarily III-V materials and  $\text{LiNbO}_3$ ) made for and during the ARO Contract. "A" means that annealing studies (temperature series) were performed (See next table for temperatures.).

ID No.	Mat'l	Dopant/SL	Source	Energy keV	Fluence $\text{cm}^{-2}$	Orient	ID	Anneal
H3118	GaAs	Si	ARDC	200	$5.0\text{E}15$	<110>		A
H3119	GaAs	Si	ARDC	200	$5.0\text{E}15$	<100>		A
H3391	GaP	S	ARDC	300	$5.0\text{E}15$	111		A
H3477	GaP	S	ARDC	333	$5.0\text{E}15$	111	-11	A
H3478	InP	S	HRL	333	$5.0\text{E}15$	100	-A	A
H3479	InP	Sn	HRL	333	$5.0\text{E}15$	100	-A	A
H3519	GaAs	Zn	Pearnton	300	$1.0\text{E}16$			A
H3534	GaAs	SL	Comas	50	$5.0\text{E}15$		711	
H3535	GaAs	SL	Comas	50	$5.0\text{E}15$		712A	A
H3590	$\text{LiNbO}_3$		U. of Glasgow	100	$1.0\text{E}16$			A
D103	GaAs		HRL	200	$3.0\text{E}15$	110		
D104	GaAs		HRL	100	$3.0\text{E}15$	110		
D105	GaAs		HRL	50	$3.0\text{E}15$	110		
D204	GaP		HRL	100	$2.0\text{E}15$	100		
D205	GaP		HRL	200	$2.0\text{E}15$	100		
D206	GaP		HRL	350	$2.0\text{E}15$	100		
D207	InP		HRL	100	$2.0\text{E}15$	110		
D208	InP		HRL	200	$2.0\text{E}15$	110		A
D209	InP		HRL	350	$2.0\text{E}15$	110		A
D210	GaP		HRL	350	$2.0\text{E}15$	111		
D211	GaP		HRL	200	$2.0\text{E}15$	111		
D212	GaP		HRL	100	$2.0\text{E}15$	111		
D213	InP		HRL	100	$2.0\text{E}15$	100		
D214	InP		HRL	200	$2.0\text{E}15$	100		
D215	InP		HRL	350	$2.0\text{E}15$	100		
D216	GaAs	Si	HRL	350	$5.0\text{E}15$	110		A
D217	GaP	S	HRL	350	$5.0\text{E}15$	111	-F A	
D218	InP	Sn	HRL	350	$5.0\text{E}15$	100	-D A	
D219	InP	S	HRL	350	$5.0\text{E}15$	100	-E A	
D226	GaSb	-	Pearnton	300	$5.0\text{E}15$			A
D227	GaAs	Zn	Pearnton	300	$5.0\text{E}15$			A
D228	GaAs	SL	NCSU	300	$1.0\text{E}16$		A 20	A
D229	He+GaAs		HRL	75	$1.0\text{E}15$		He 123	A
D230	GaAs/Si	Si	Spire/ARDC	100	$5.0\text{E}15$		MOCVD 10236	A
D231	InSb		Pearnton	300	$5.0\text{E}15$			A
D232	AlAs/GaAs	SL	Novak	300	$5.0\text{E}15$			
D239	InSb/GaAs	SL	Comas	300	$5.0\text{E}15$	$\text{LN}_2$	971	A
D240	InSb		Pearnton	300	$5.0\text{E}15$	$\text{LN}_2$	(see D231)	A
D241	GaAs	none	LEC	300	$5.0\text{E}15$		1000s	A
D245	InSb/GaAs	SL	Comas	200	$5.0\text{E}15$	NG		
D247	GaAsP		Novak	150	$5.0\text{E}15$			
D281	$\text{LiNbO}_3$		HRL	100	$5.0\text{E}15$			A
D282	$\text{LiNbO}_3$		U. of Glasgow	100	$1.0\text{E}16$			

D283	GaP	Zn	Pearton	300	8.5E15			A
D284	GaP	S	HRL	300	8.5E15			A
D285	InP	S	HRL	300	8.5E15			A
D286	InAs		Pearton	300	8.5E15			A
He123	GaAs		HRL	300	3.0E15	100		
He126	GaAs		HRL	200	3.0E15	100		
He131	GaP		HRL	100	3.0E15	111		
He136	GaP		HRL	200	3.0E15	111		
He137	InP	?	HRL	350	5.0E15	100	-B	A
He138	GaP	S	HRL	350	5.0E15	111	-D	A
He139	InP	Sn	HRL	350	5.0E15	100	-B	A
Be2579	GaP, InP		HRL	100	5.0E12			A
Be2580	GaP, InP		HRL	100	1.0E14			A
Be2608	GaAs	SL	Comas	170	2.0E14		712B	A
Be2666	AR0	SL	Novak	700	1.3E13			
Be3312	GaAsP		Novak	350	2.0E13			A
Be3316	InP	Fe	HRL	700	1.3E13			A
Be3317	GaSb		Pearton	700	1.3E13			A
Be3318	LiNbO <sub>3</sub>		Xtal Technol	700	1.3E13			A
Be3319	GaAs		Airt	700	1.3E13			A
Be3322	GaP	S		700	1.3E13			A
Be3323	InSb		Pearton	700	1.3E13			A
Be3348	InAs		Pearton	200	1.0E14			
C228-240(part)	various		HRL	100	2.0E13			
				200	2.0E13			
				400	2.0E13			
				700	2.0E13			
0886-932(part)	various		HRL	100	2.0E13			
				200	2.0E13			
				400	2.0E13			
				700	2.0E13			
Mg289-292(part)	various		HRL	250	1.0E14			
Si9171	GaSb		Pearton	150	2.0E13			
Si9500	GaAsP		Novak	300	1.0E14			A
Si9667	InAs		Pearton	28 180	1.0E14			
Si9667	InP		HRL	+30 180	2.0E14			A
S976-1027(part)	various		HRL	100	2.0E13			
				200	2.0E13			
				400	2.0E13			
				700	2.0E13			
Zn157-171(part)	various		HRL	200	2.0E13			
				400	2.0E13			

Se577-588(part)	various	HRL	200	4.0E12
			200	1.0E14
			400	4.0E12
			400	1.0E14
Se589-602(part)	various	HRL	200	2.0E13
Se634-640(part)	various	HRL	400	1.0E14
Cd298-301(part)	various	HRL	500	1.0E14
Y2-3	GaAs, InP	HRL	300	1.0E14
La2-3	GaAs, InP	HRL	300	1.0E14
Nd2-3	GaAs, InP	HRL	300	1.0E14
Sm2-3	GaAs, InP	HRL	300	1.0E14
Er2-3	GaAs, InP	HRL	300	1.0E14
Yb2-3	GaAs, InP	HRL	300	1.0E14

#### MeV Implants

MeV H	LiNbO <sub>3</sub>	Xtal Technol	1000	3.0E15	A
	GaAs(Si)	ARC	1000	3.0E15	A
	GaP(S)	HRL	1000	3.0E15	A
	InP(S)	HRL	1000	3.0E15	A
	InP(Fe)	HRL	1000	3.0E15	A
	InSb	ATT	1000	3.0E15	A
MeV He	GaAs		2000	5.0E15	A
	GaP	"	2000	5.0E15	A
	InP		2000	5.0E15	A
	LiNbO <sub>3</sub>		2000	5.0E15	A
MeV Si	GaAs		2000	2.0E14	A
	GaP	"	2000	2.0E14	A
	InP		2000	2.0E14	A
	InSb		2000	2.0E14	A
	LiNbO <sub>3</sub>		2000	2.0E14	A
MeV Ge	GaAs		2400	1.0E15	A
	GaP	"	2400	1.0E15	A
	InP		2400	1.0E15	A
	InSb		2400	1.0E15	A

Be2534-56	-783, 847R1, -932, -933, 934, 848, 849, -841, -787, 846R1, 935, 845, 930
Be2608	-909
Be2579	844R1
Be2580	845, 846R1
Be3316 InP	-1088
Be3317 GaSb	-1091
Be3318 LiNbO <sub>3</sub>	-1099
Be3319 GaAs	-1089
Be3322 GaP	-1090
Be3323 InSb	-1091
Si9500	-1092
Se	-928(GaP)
MeV Si(6)	-942, -1098
MeV Ge(2.4)	-949(GaP), -950, -951
AlGaAs SL	-914

# Summary of Implants by Material

GaAs (p)	H3519	D227		
GaAs (n)	H3118, H3119, MeV H	D216		
GaAs	D229, D241, He123, Be3319			
	Y2-3, La2-3, Nd2-3, Sm2-3, Er2-3, Yb2-3			
GaP (p)		D283		
GaP (n)	H3391, H3477, MeV H	D217, D284	Be2579,80	
	He138		Be3322	
InP (p)				
InP (n)	H3478, H3479, MeV H	D208, D209, D218, D219, D285		
	He139			
InP (- or Fe)	He137, Be2573, Be2580, Be3316, Si9667			
	Y2-3, La2-3, Nd2-3, Sm2-3, Er2-3, Yb2-3			
InAs	MeV H	D286	Be3348	Si9667
GaSb		D226	Be3317	Si9171
InSb	MeV H	D231, D240	Be3323	
GaAs/Si	D230			
GaAsP		D247	Be3312	Si9500
AlGaAs SLs	H3534	D228, D232	Be2608, Be2666	
InSb/GaAs SLs	H3535, MeV H	D239, D245		
LiNbO <sub>3</sub>	H3590, MeV H	D281, D282	Be3318	

# Summary of Annealing Temperatures

Temperatures (in °C) done as part of annealing studies performed  
for the samples listed in the Implant Summary table.

H3391	100, 200, 300, 400, 500, 600	
H3477	300, 325, 350, 375, 400, 450, 500	
H3478	300, 325, 350, 375, 400, 450, 500, 550, 600	
H3479	300, 325, 350, 375, 400, 450, 500, 550, 600	
H3519	100, 200, 300, 350, 400, 450, 500, 600	
H3535	300, 500	
H3590	250, 300, 350, 400	
H 1.0 MeV set	300, 500	
D216	350, 400, 450, 500	
D217	300, 325, 350, 375, 400, 450, 500, 550, 600	+350, 500 FL
D218	275, 300, 325, 350, 375, 400, 450, 500, 550, 600	+350, 500 FL
D219	275, 300, 325, 350, 375, 400, 450, 500, 550, 600	
D226	200, 225, 250, 275, 300, 400, 500, 600	
D227	200, 250, 300, 350, 400, 500, 600, 700	
D228	200, 300, 400, 500, 600, 700	
D229	(He123) 300, 500	
D230	200, 300, 400, 500, 600	
D231	100, 150, 175, 200, 225, 250, 275, 300, 400, 500	
D239	150, 200, 250, 300	
D240	100, 125, 150, 175, 200, 300, 400, 500	
D241	200, 250, 300, 350, 400, 450, 500, 550, 600, 700	
D281	250, 300, 350, 400	
D282	300, 500, 700	
D283	300, 350, 400, 500, 600, 700	
D284	300, 500, 700	
D285	300, 500, 700	
D286	300, 500, 700	

He 2.0 MeV set 300

Be profiles in annealed SL 712B

Be2608 300, 500, 550, 600

Be set at 700 keV 750

Si MeV set 750

Summary of Implant/Annealing/SIMS Profiling Studies  
by Implant/Sample Number

H3118 GaAs 200 keV  $5.0 \times 10^{15} \text{ cm}^{-2}$   $\langle 110 \rangle$  CH Annealed 300, 500°C

H3119 GaAs 200 keV  $5.0 \times 10^{15} \text{ cm}^{-2}$   $\langle 100 \rangle$  CH Annealed 300, 500°C

This experiment was performed to determine how channeled implants or channeled depth distributions redistribute upon annealing - whether they redistribute differently from random implant profiles. Both show good redistributed profiles for 300°C anneal - both deeper and toward the surface; the  $\langle 100 \rangle$  profiles are like the random profiles, but the  $\langle 110 \rangle$  shallow, toward the surface profile is somewhat different, as if there were less effect of damage, which there should be because the implant was channeled. The deep diffused profile is displaced deeper for the  $\langle 110 \rangle$  implant, essentially by the deeper channeled beginning location of the H depth distribution for the diffusion. For 500°C, the H profiles are just detectable, that is, nearly gone in both crystal orientations, but visible after background subtraction in the region of the peak of the original profile.

H3535 AR0 Superlattice 712 (Comas) implanted with  $5.0 \times 10^{15} \text{ cm}^{-2}$  50 keV  $^1\text{H}$ . Annealed at 300 and 500°C.

H3477 GaP(S) Implanted with  $5 \times 10^{15} \text{ cm}^{-2}$  333 keV  $^1\text{H}$ . Annealed at 350, 375, 400, 450, 500°C. The deep H diffusion profiles are just great enough in density to detect, using background subtraction ( $10^{17}$ - $10^{18} \text{ cm}^{-3}$ ). The shallow redistribution toward the surface begins at 375°C and is quite high in density ( $>10^{19} \text{ cm}^{-3}$ ) even to 500°C. Thus GaP retains H in this region to annealing temperature of greater than 500°C.

H3478 InP(S) Implanted with  $5 \times 10^{15} \text{ cm}^{-2}$  333 keV  $^1\text{H}$ . Annealed at 325,  
H3479 InP (Sn) 350, 375, 400, 450, 500, 550, 600°C. Both n-type. Both  
same H profiles. The deep H diffusion profile in both is too low in  
density to detect ( $< 10^{17} \text{ cm}^{-3}$ ). The shallow redistribution toward the  
surface is easily detected - H density between  $10^{19}$  and  $10^{17} \text{ cm}^{-3}$ . H  
reaches the surface at 375°C, and then decreases to  $< 10^{17} \text{ cm}^{-3}$  by  
600°C.

H3519 GaAs(Zn) from Pearton implanted with  $1.0 \times 10^{16} \text{ cm}^{-2}$  333 keV  $^1\text{H}$ .  
Annealed at 100, 200, 300, 350, 400, 450, 500, and 600°C. Shows the  
redistribution of H toward the surface and deeper into the bulk,  
because the Zn-doped p-type GaAs retains H at a much higher density  
-- above the detection limit of SIMS for  $^1\text{H}$ . The H does not  
disappear from the GaAs until 600°C is reached.

H3535 Comas AlGaAs/GaAs superlattice 712, implanted with  $5 \times 10^{15} \text{ cm}^{-2}$  50-keV  
 $^1\text{H}$  and annealed at 300 and 500°C. Shows the Al layer oscillations,  
the H profiles, and H decoration of the strain or dislocations at the  
superlattice/substrate interface. H is nearly gone in the SL at  
500°C, but remains at the buffer layer/substrate interface.

D208 840 Comb of -838 and -839

D214 840

D213 100 keV InP from HRL implanted with  $2.0 \times 10^{15} \text{ cm}^{-2}$   $^2\text{H}$ .

D214 200 keV An energy set.

D215 350 keV Profile parameters shown below for 200 and 350 keV.

	200 keV	350 keV
$R_m \text{ } \mu\text{m}$	1.96	3.34
$R_p \text{ } \mu\text{m}$	1.90	3.28
$\Delta R_p \text{ } \mu\text{m}$	0.216	0.296
$\gamma_1$	-1.26	-0.83
$\beta_2$	6.91	5.68
$\beta_2'$	0.91	0.68
$N_{max} \text{ cm}^{-3}$	$4.6 \times 10^{19}$	$4.8 \times 10^{19}$

- D226 GaSb material from S. Pearton of AT&T Bell Labs, implanted with  $5 \times 10^{15} \text{ cm}^{-2}$  300-keV  $^2\text{H}$  and annealed at 100, 200, 225, 250, 275, 300, 350, 400, and 500°C. H redistribution, beginning at 200°C, is shown to progress deeper into the substrate with increasing annealing temperature; the H is gone for the 400 and 500°C temperatures.
- D227 GaAs(Zn) material from S. Pearton of AT&T Bell Labs, implanted with  $5 \times 10^{15} \text{ cm}^{-2}$  300-keV  $^2\text{H}$  and annealed at temperatures of 100, 200, 300, 400, 500, 600, and 700°C. The H redistribution is generally the same, except in the region of heaviest implant damage, under the peak of the implant, where several peaks or an oscillation in the H profile is seen.
- D229 LEC GaAs from HRL implanted with  $5 \times 10^{15} \text{ cm}^{-2}$  300-keV He, and subsequently implanted with  $1 \times 10^{15} \text{ cm}^{-2}$  75-keV  $^2\text{H}$  and annealed at 300 and 500°C. No redistribution occurs for 300°C, but for 500°C, the H decorates the damage from the He implant, with some structure.
- D230 MOCVD epi GaAs on Si, doped with Si, from Spire Corp. via S. Pearton of AT&T, implanted with  $5 \times 10^{15} \text{ cm}^{-2}$  100-keV  $^2\text{H}$ , and annealed at 200, 300, 400, 500, 600, and 700°C. The Si profile through the GaAs layer was measured. The H redistributes beginning above 200°C, and decorates the strain or dislocations at the GaAs/Si interface. H is still present in the GaAs layer, but at reduced density, after 700°C.
- D231 InSb from S. Pearton of AT&T Bell Labs,  $\sim 50^\circ\text{C}$  implanted with  $5 \times 10^{15} \text{ cm}^{-2}$  300-keV  $^2\text{H}$ , and annealed at 200, 250, 300, and 350°C. All temps show redistribution, even the as-implanted sample. H is gone (beneath detection limit) by 350°C. See D240.
- D240 Same as D231, except implanted at  $-150^\circ\text{C}$ , and annealed at 125, 150, and  $175^\circ\text{C}$ . H redistributes more like in GaAs - toward surface and deeper with increasing temperature.
- D241 GaAs(Si) from AR0. Implanted with  $5 \times 10^{15} \text{ cm}^{-2}$  300 keV  $^2\text{H}$ . Annealed at 200, 300, and 400°C.

- D245 InSb/GaAs MBE superlattice from J. Comas of NRL/NBS (972,973: 10 and 20 nm layers of  $1.5\mu\text{m}$  total thickness), implanted with  $5 \times 10^{15} \text{ cm}^{-2}$  200-keV  $^2\text{H}$ , and not yet annealed. We have not been successful in measuring the alternate layers of this difficult structure using low energy (1.5 keV) O SIMS, so disordering cannot be studied.
- D281  $\text{LiNbO}_3$  from HRL implanted with  $5.0 \times 10^{15} \text{ cm}^{-2}$  100 keV  $^2\text{H}$  and annealed at 300, 350, 400, and  $450^\circ\text{C}$ . These profiles show the striking redistribution of H in  $\text{LiNbO}_3$  that include the "uphill" diffusion and the high density of H in diffused  $\text{LiNbO}_3$   $> 10^{18} \text{ cm}^{-3}$ .
- D282  $\text{LiNbO}_3$  from Univ. of Glasgow implanted with  $1.0 \times 10^{16} \text{ cm}^{-2}$  100 keV  $^2\text{H}$ . This implant served as the SIMS standard for quantification of the H SIMS profiles in the Univ. of Glasgow hydrogen exchanged and annealed  $\text{LiNbO}_3$  work.
- D283 GaP(Zn) from S. Pearton of ATT Bell Labs. Implanted with  $8.5 \times 10^{15} \text{ cm}^{-2}$  300 keV  $^2\text{H}$ . Annealed at 300, 350, 400, 500, 600, and  $700^\circ\text{C}$ . Shows H redistribution well because it is Zn-doped p-type GaP, which retains a high density of H. More anneal temperatures are being done now and the set will be completed after this report is submitted. These results should be published.
- D284 GaP(S) from HRL. Implanted with  $8.5 \times 10^{15} \text{ cm}^{-2}$  300 keV  $^2\text{H}$ . Annealed at 300, 500, and  $700^\circ\text{C}$ . Shows H redistribution but at lower density than D283.
- D285 InP(S) from HRL. Implanted with  $8.5 \times 10^{15} \text{ cm}^{-2}$   $^2\text{H}$ . Annealed at 300, 500, and  $700^\circ\text{C}$ . MORE. Also, S was profiled under the  $^2\text{H}$  implant for the 300 and  $500^\circ\text{C}$  anneals. S shows oscillations of  $\sim 1\mu\text{m}$  period that may be S decoration of strain induced in the InP crystal during LEC growth as the temperature controller cycles and the temperature varies periodically very slightly.
- D286 InAs from S. Pearton of ATT Bell Labs. Implanted with  $8.5 \times 10^{15} \text{ cm}^{-2}$  300 keV  $^2\text{H}$ . Annealed at 300, 500, and  $700^\circ\text{C}$  MORE